Arabian Journal of Chemistry (2022) **15**, 103504

King Saud University

**Arabian Journal of Chemistry**

www.ksu.edu.sa
www.sciencedirect.com

ORIGINAL ARTICLE

# Design, synthesis and biological evaluation of novel 2-phenyl-4,5,6,7-tetrahydro-1*H*-indole derivatives as potential anticancer agents and tubulin polymerization inhibitors

**Guangcheng Wang [a,*], Min He [a,d], Wenjing Liu [a,d], Meiyan Fan [a,d], Yongjun Li [c], Zhiyun Peng [b,*]**

[a] *State Key Laboratory of Functions and Applications of Medicinal Plants, Guizhou Provincial Key Laboratory of Pharmaceutics, Guizhou Medical University, Guiyang, China*
[b] *College of Food Science and Technology, Shanghai Ocean University, Shanghai, China*
[c] *Engineering Research Center for the Development and Application of Ethnic Medicine and TCM (Ministry of Education), Guizhou Medical University, Guiyang, China*
[d] *Teaching and Research Section of Natural Medicinal Chemistry, School of Pharmacy, Guizhou Medical University, Guiyang, China*

Received 5 September 2021; accepted 12 October 2021
Available online 22 October 2021

**KEYWORDS**

Tetrahydro-1*H*-indole;
Hydrazone;
Tubulin polymerization inhibitors;
Anticancer activity

**Abstract** A new series of 2-phenyl-4,5,6,7-tetrahydro-1*H*-indole derivatives as tubulin polymerization inhibitors were synthesized and evaluated for the anti-proliferative activities. All newly prepared compounds were tested for their antiproliferative activity *in vitro* on the human breast cancer cell line (MCF-7) and human lung adenocarcinoma cell line (A549). Among them, compound **7b** with a 4-methoxyl substituent at the phenylhydrazone moiety exhibited the most potent anticancer activity against MCF-7 and A549 with $IC_{50}$ values of 1.77 ± 0.37 and 3.75 ± 0.11 μM, respectively. Interestingly, **7b** displayed significant selectivity in inhibiting cancer cells over LO2 (normal human liver cells). Further mechanism studies revealed that **7b** significantly arrested cell cycle at G2/M phase and induced apoptosis in a dose-dependent manner. Additionally, **7b** effectively inhibited tubulin polymerization with an inhibitory manner similar to that of colchicine. Furthermore, molecular docking study suggested that **7b** had high binding affinities for the colchi-

* Corresponding Author.
E-mail addresses: wanggch123@163.com (G. Wang), pengzhiyun1986@163.com (Z. Peng).
Peer review under responsibility of King Saud University.

Production and hosting by Elsevier

https://doi.org/10.1016/j.arabjc.2021.103504

cine binding pocket of tubulin. Hence, this study demonstrates for the first time that tetrahydroindole can be used as a functional group for the design and development of new tubulin polymerization inhibitors.



## 1. Introduction

Microtubules are key components of the cytoskeleton in eukaryotic cells, which mainly consist of α- and β-tubulin heterodimers (Downing & Nogales, 1998a, 1998b). They play important roles in a series of essential cellular processes including intracellular transportation, regulation of motility, cell signaling, formation and maintenance of cell shape, and secretion (Honore et al., 2005). It was found that the formation of microtubules is a dynamic process related to the polymerization and depolymerization of α- and β-tubulin heterodimers (Amos, 2004). The interruption of the dynamic equilibrium of α- and β-tubulin heterodimers hinders cell division at mitosis and thus resulting in cell cycle arrest at metaphase, which leads to the tumor cell death by apoptosis (Jordan et al., 1996). Hence, microtubules have become one of the most successful therapeutic targets for the treatment of human cancer (Dumontet & Jordan, 2010; Jordan & Wilson, 2004; Stanton et al., 2011).

Pyrroles are an important class of nitrogen-containing heterocyclic compounds, which are present in numerous naturally occurring and synthetic compounds, such as Vitamin B12, Chlorophyll, Tolmetin, Zomepirac, Pyrvinium, and Prodigiosin (Ahmad et al., 2018; Singh et al., 2021). Previous studies revealed that pyrrole derivatives exhibit a wide range of pharmacological activities including anticancer, antimalarial, anti-HIV, anti-inflammatory, anti-depressant, and anti-ulcer activities (Ahmad et al., 2018). Specifically, pyrrole fused form indole is a very common skeleton in natural products and synthetic compounds, which have attracted great attention in medicinal chemistry over the past decade (Singh & Singh, 2018; Sravanthi & Manju, 2016). It is interesting to point that indole has been proven to be an important pharmacophore for the design and development of anticancer agents and tubulin polymerization inhibitors (Patil et al., 2016; Sang et al., 2017; Sunil & Kamath, 2016; Wan et al., 2019). Over the last few years, numbers of indole-containing tubulin polymerization inhibitors have been used in clinical (vinblastine and vincristine) or in clinical trials (indibulin, MKC-118, and LP-261) (Wang et al., 2014).

In recent years, tetrahydroindole derivatives have aroused increased interest due to their enhanced biological activity. For instance, Vojacek et al. found that 2,6,6-trimethyl-4-oxo-4,5,6,7-tetrahydro-*1H*-indole-3-carboxamides are potent and selective SIRT2 inhibitors, and could serve as an exquisite starting point for hit-to-lead profiling (Fig. 1, **I**) (Vojacek et al., 2019). Andreev et al. discovered that the 2-phenyl-4,5,6,7-tetrahydro-*1H*-indole could be used as a novel anti-hepatitis C virus targeting scaffold (Fig. 1, **II**) (Andreev et al., 2015). Sun et al. reported that a series of new 3-substituted indolin-2-one derivatives containing a tetrahydroindole moiety (Fig. 1, **III**) can be used as specific inhibitors of receptor tyrosine kinases (Sun et al., 2000). Fatahala et al reported the synthesis of a series of tetrahydroindole derivatives and some of them shown promising antioxidant activity besides their anticancer activity (Fig. 1, **IV**) (Fatahala et al., 2015). Recently, Gülçin et al. reported the synthesis of sulfur-containing tetrahydroindole derivatives (Fig. 1, **V** and **VI**) which showed excellent inhibitory potential against the human erythrocyte carbonic anhydrase I, and II isoenzymes, acetylcholinesterase (AChE), butyrylcholinesterase (BChE), and α-glycosidase enzymes (Gulcin et al., 2020).

However, to the best of our knowledge, there is no report about tetrahydroindole derivatives as tubulin polymerization inhibitors. Hence, prompted by these observations and in continuation to our interest in design and synthesis of novel tubulin polymerization inhibitors (Wang et al., 2020a, Wang et al., 2020c, Wang et al., 2020d; Wang et al., 2018a; Wang et al., 2018b), herein we report for the first time the synthesis of a novel series of 2-phenyl-4,5,6,7-tetrahydro-1*H*-indole derivatives as potential anticancer agents and tubulin polymerization inhibitors. The mechanism of antiproliferative effects of this class of compounds was studied by using *in vitro* tubulin polymerization, cell cycle arrest, and cell apoptosis assay. Furthermore, molecular modeling study was also performed to elucidate the binding mode of the inhibitor with tubulin.

## 2. Results and discussion

### 2.1. Synthesis

A novel series of 2-phenyl-4,5,6,7-tetrahydro-1*H*-indole derivatives **7a-7o** were synthesized according to the pathways described in Schemes 1. The commercially available 1-pyrrolidinocyclohexene **1** was reacted with 2-bromo-1-(4-meth oxyphenyl)ethan-1-one **2** (commercially from Bide Pharm) in DMF and then hydrolyzed at room temperature to give the corresponding **3** (Naik et al., 2014). The subsequent cyclization of **3** with $NH_4Ac$ under reflux in EtOH as a solvent to generate 2-(4-methoxyphenyl)-4,5,6,7-tetrahydro-1*H*-indole **4**. Then, according to Duff reaction, intermediate **4** reacted with hexamethylenetetramine under reflux in acetic acid to afford the key intermediate **5**. Finally, condensation of intermediate **5** with appropriate benzoyl hydrazines **6a-6o** in the presence of acetic acid in ethanol to afford the title compounds (**7a-7o**) in high yields (69%-87%).

The chemical structures of these title compounds were characterized by spectroscopic methods ($^1$H NMR and $^{13}$C NMR), as well as HRMS spectrometry (see **Supporting Information**). Such as the $^1$H NMR spectrum of **7b** shown two singlets at $\delta$ 3.80 and 3.81 ppm due to two methoxy groups on the benzene ring. The methylene protons (–$CH_2$–) of tetrahydroindole moiety were appeared at $\delta$ 1.72–1.75 (m, 4H), 2.56 (t, 2H, $J$ = 6.8 Hz) and 2.73 ppm (t, 2H, $J$ = 6.8 Hz). Four doublet

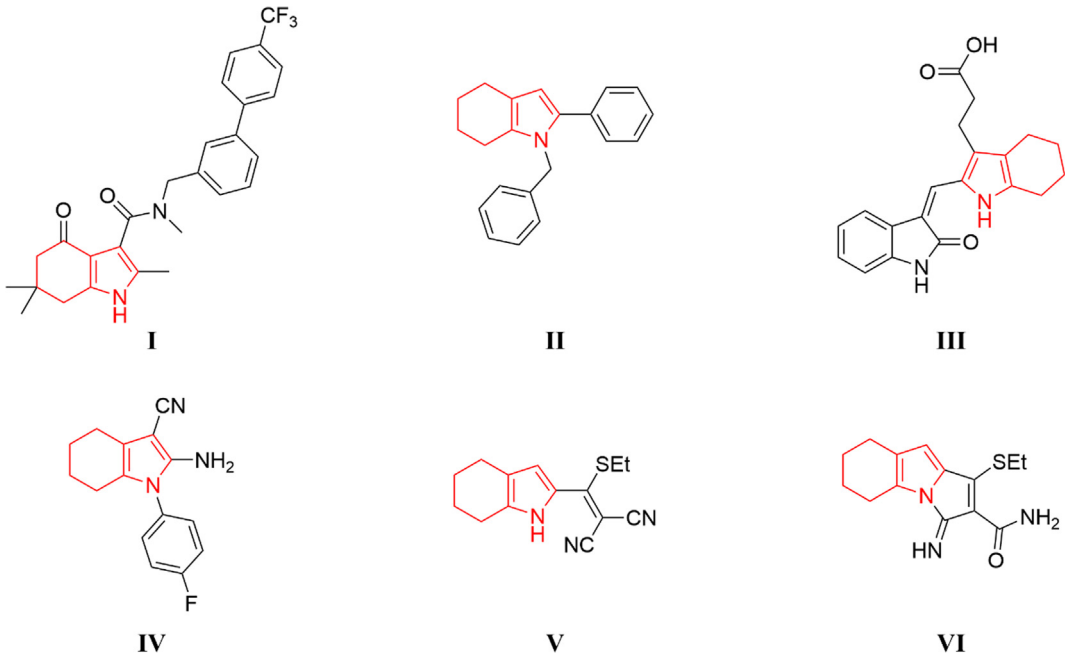


**Fig. 1** Some tetrahydroindole derivatives with diverse pharmacological activities.

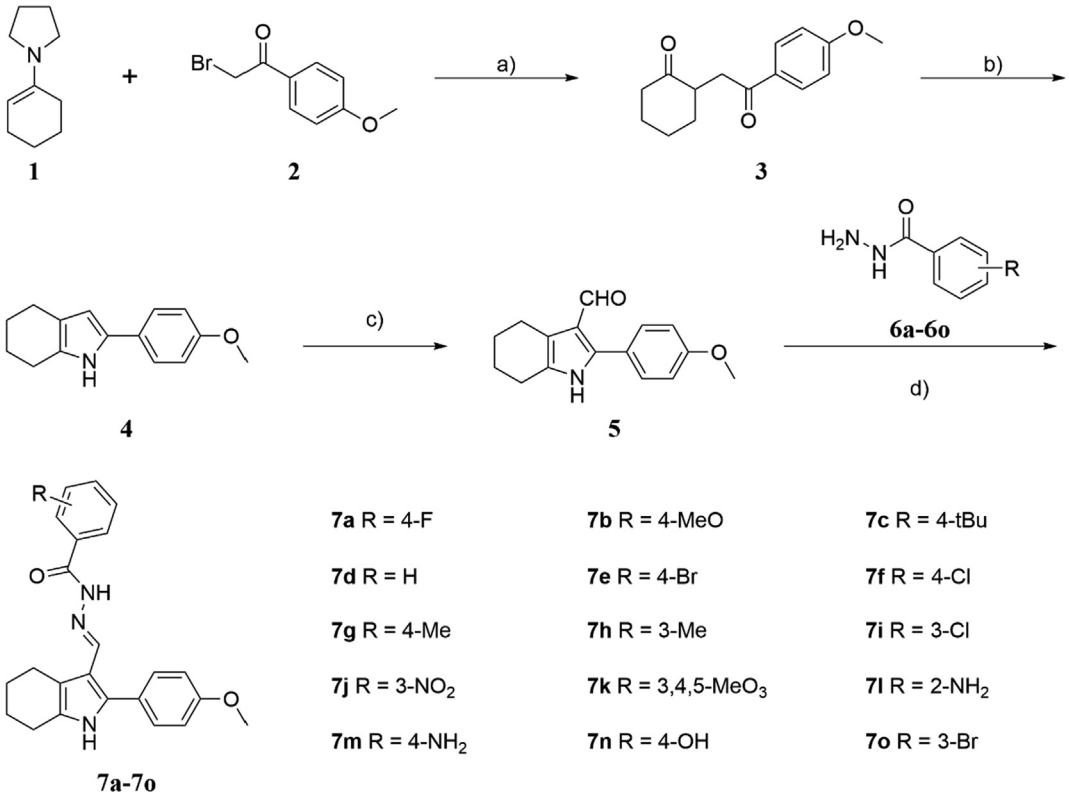


**Scheme 1** (a) DMF, room temperature, 4 h, then $H_2O$, room temperature, 12 h; (b) $NH_4Ac$, EtOH, reflux, 1 h; (c) hexamethylenetetramine, AcOH, reflux, 3 h; (d) AcOH (c), EtOH, reflux, 5 h.

peaks at $\delta$ 7.00, 7.02, 7.34 and 7.84 ppm with coupling constant of 8.4 Hz were attributed to two 4-methoxybenzyl parts. The singlet peak of CH proton of hydrazone moiety was observed at 8.44 ppm, and the signals of NH were shown as two single peaks at $\delta$ 10.88 and 11.14 ppm. In $^{13}C$ NMR spectrum of **7b** the signals at $\delta$ 22.84, 23.25, 23.83 and 24.33 ppm were assigned to the methylene carbon in tetrahydroindole moiety. The signals at $\delta$ 55.76 and 55.88 ppm were

attributed to the carbon in two methoxyl groups. The multiple signals observed at $\delta$ 113.51–133.64 ppm were assigned to aromatic ring. The signals observed at $\delta$ 146.21 ppm was assigned to CH carbon of hydrazone moiety. The signals at $\delta$ 158.89–162.11 ppm attributed to carbonyl group or the aromatic carbon connected with the methoxy. The high-resolution mass spectrum of **7b** shown a molecular ion peak at *m/z* 404.1847 as $[M-H]^-$. Therefore, the spectral data ($^1$H NMR, $^{13}$C NMR, and HRMS) were in full agreement with the expected structure of the compound **7b**.

### 2.2. Biological evaluation

#### 2.2.1. In vitro anticancer activity and cytotoxicity

The growth inhibitory effects of the newly synthesized 2-phenyl-4,5,6,7-tetrahydro-1*H*-indole derivatives **7a-7o** were evaluated for their *in vitro* cytotoxicity profiles against human breast cancer cell line (MCF-7) and human lung adenocarcinoma cell line (A549) using the CCK-8 assay with cisplatin, 5-fluorouracil (5-Fu), tamoxifen, and combretastatin A-4 (CA-4) as reference standards. The $IC_{50}$ values (50% inhibitory concentrations) of all the tested compounds for both cancer cell lines are summarized in Table 1. In comparison to the standard drug cisplatin, 5-Fu, tamoxifen, and CA-4, all tested compounds showed potent antiproliferative activity on the MCF-7 and A549 cancer cell lines with $IC_{50}$ ranging from 1.77 ± 0.37–4.73 ± 0.61 μM and 3.74 ± 0.21–7.47 ± 0.57 μM, respectively. Among the series, compound **7b** with a 4-methoxyl substituent at the phenylhydrazone moiety exhibited the most potent anticancer activity against MCF-7 and A549 with $IC_{50}$ values of 1.77 ± 0.37 and 3.75 ± 0.11 μM, respectively. These results indicated that 4-methoxy group plays an important role in the improvement of antiproliferative activity for this class of compounds, which was consistent with the previously reported study (Li et al., 2017; Xia et al., 2020). The replacement of 4-methoxy group with other substituents (F, Cl, Br, Me, tBu, etc) resulted in a slight decrease in antiproliferative activity. It is particularly noteworthy that although 3,4,5-trimethoxy fragment has been proved to be the optimal group for tubulin inhibitors (Li et al., 2018). Many tubulin inhibitors contain this fragment in their structure. However, the replacement of 4-methoxy group (**7b**) with 3,4, 5-trimethoxy (**7 k**) resulted in a slight decrease in antitumor activity on MCF-7 cells, but a significant decrease in antitumor activity on A549 cells.

In order to evaluate the safety of these new synthetic compounds, we selected the most active compound **7b,** and tested its toxicity to human normal liver cell line (LO2). The result was shown that **7b** displayed moderate cytotoxicity against LO2 with an $IC_{50}$ value of 44.71 ± 2.71 μM. Due to compound **7b** exhibited strong antiproliferative activity against human cancer cell lines with $IC_{50}$ values of 1.77 ± 0.37 (MCF-7) and 3.75 ± 0.11 μM (A549), respectively. These results indicated that compound **7b** showed higher selectivity to tumor cells than normal cells. Hence, it can be concluded that these compounds have good safety for potential application in the treatment of human cancer.

**Table 1** The *in vitro* antiproliferative activities of compounds **7a-7o** against human cancer cell lines.

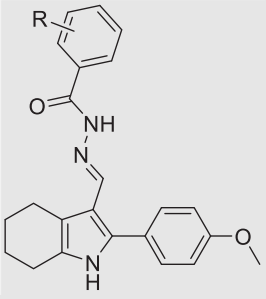


| Compound | R | $IC_{50}$ (μM)[a] | |
|---|---|---|---|
| | | MCF-7 | A549 |
| **7a** | 4-F | 3.63 ± 0.39 | 4.12 ± 0.29 |
| **7b** | 4-MeO | 1.77 ± 0.37 | 3.75 ± 0.11 |
| **7c** | 4-tBu | 4.73 ± 0.61 | 6.68 ± 0.27 |
| **7d** | H | 2.21 ± 0.54 | 3.08 ± 0.66 |
| **7e** | 4-Br | 3.50 ± 0.50 | 7.17 ± 0.33 |
| **7f** | 4-Cl | 3.30 ± 0.38 | 4.38 ± 0.12 |
| **7 g** | 4-Me | 2.97 ± 0.78 | 4.04 ± 0.13 |
| **7 h** | 3-Me | 3.54 ± 0.56 | 3.93 ± 0.16 |
| **7i** | 3-Cl | 4.04 ± 0.44 | 7.18 ± 0.90 |
| **7j** | 3-$NO_2$ | 3.03 ± 0.32 | 4.68 ± 0.06 |
| **7 k** | 3,4,5-$MeO_3$ | 2.07 ± 0.17 | 7.47 ± 0.57 |
| **7 l** | 2-$NH_2$ | 2.33 ± 0.40 | 7.40 ± 0.45 |
| **7 *m*** | 4-$NH_2$ | 1.90 ± 0.31 | 3.74 ± 0.21 |
| **7*n*** | 4-OH | 2.21 ± 0.17 | 7.42 ± 0.11 |
| **7o** | 3-Br | 4.02 ± 0.18 | 5.09 ± 0.40 |
| **Cisplatin** | – | 11.15 ± 0.75 | 4.92 ± 0.56 |
| **5-Fu** | – | 11.61 ± 0.60 | 2.75 ± 0.31 |
| **Tamoxifen** | – | 14.28 ± 0.40 | 20.20 ± 0.65 |
| **CA-4** | – | 5.55 ± 0.11 | 0.029 ± 0.004 |

[a] The values given are means of three experiments.

#### 2.2.2. Cell cycle analysis

Encouraged by the preliminary *in vitro* antiproliferative screening results, the anticancer mechanism of this series of compounds was further explored, the most potent compound **7b** was selected to investigate its effect on the cell cycle progression of MCF-7 cancer cells using flow cytometry analysis. In this study, MCF-7 cancer cells were treated with DMSO (control group) or increased concentrations of **7b** (0.625, 1.25, and 2.5 μM) for 24 h. As depicted in Fig. 2, the percentage of cells at the G2/M phase in presence of the compound was 30.67%, 42.24%, and 71.31%, respectively, while 25.98% of the G2/M phase was detected for the control group. These findings demonstrated that compound **7b** concentration-dependently caused a significant G2/M arrest, which was a representative characteristic for tubulin polymerization inhibitors (Wang et al., 2021; Wang et al., 2020b).

#### 2.2.3. Cell apoptosis study

Due to breast cancer is the most common invasive cancer in women, and many tubulin polymerization inhibitors are commonly used in clinical for the treatment of breast cancer, we selected MCF-7 cells to evaluate the antitumor activity of these compounds. It has been demonstrated that tubulin polymerization inhibitors are able to induce cellular apoptosis (Mustafa et al., 2019; Wang et al., 2020c), we also examined whether compound **7b** can induce cell apoptosis. In this work,

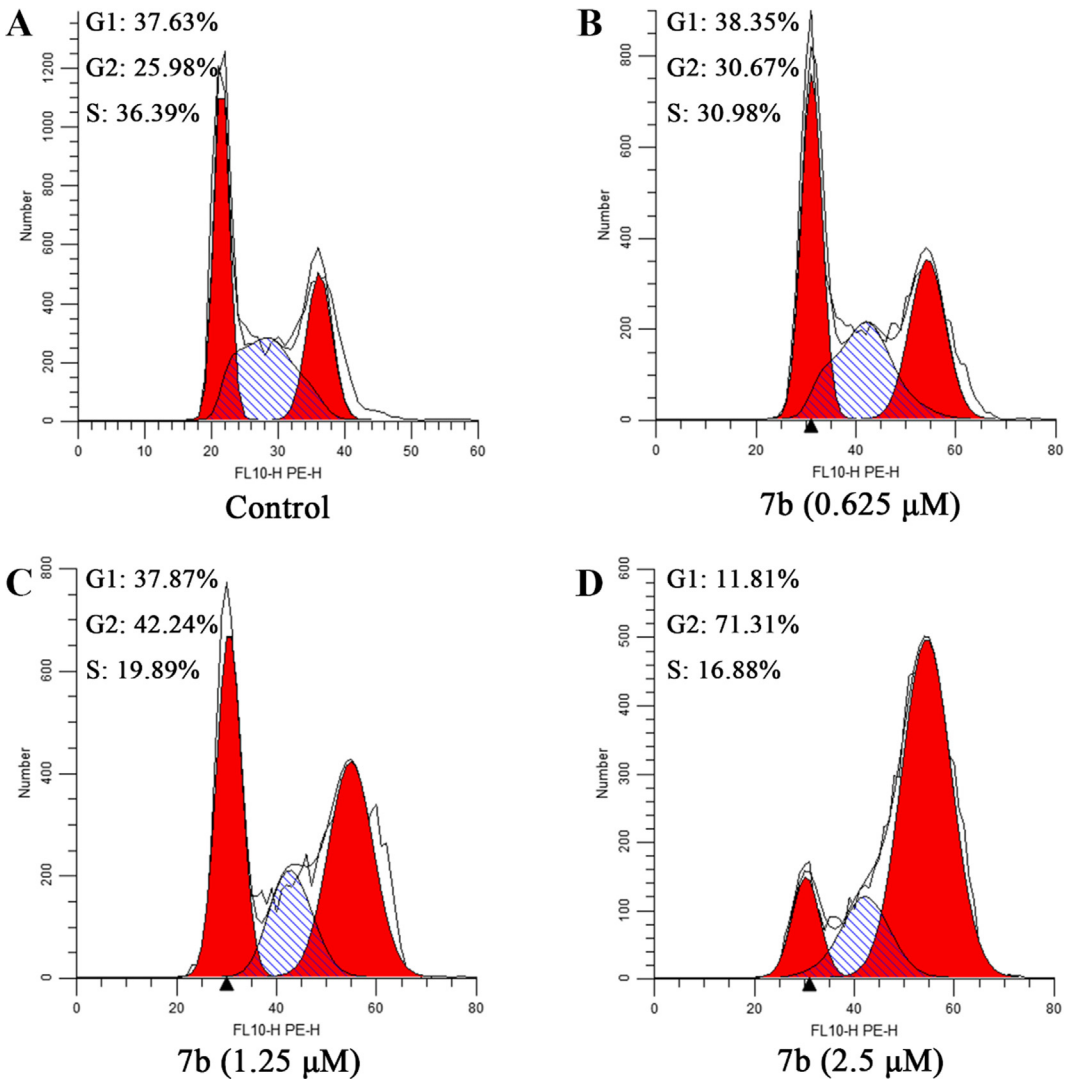


**Fig. 2** Effect of compound **7b** on cell cycle in MCF-7 cells. Flow cytometry of MCF-7 cells treated with **7b** for 24 h. (A) Control; (B) **7b**, 0.625 μM; (C) **7b**, 1.25 μM; (D) **7b**, 2.5 μM.

cell apoptosis analysis of MCF-7 cells incubated with the increasing concentrations of **7b** (0.5, 2.0, and 5.0 μM) was performed using an Annexin V-FITC/PI assay. As shown in Fig. 3, after treatment with **7b** at the concentrations of 0.5, 2.0, and 5.0 μM for 24 h, the total numbers of early (Q3) and late apoptotic (Q2) cells were 28.4%, 31.4%, and 53.3%, respectively, whereas that of the control group was only 9.21%. Hence, the results revealed that compound **7b** exhibited antiproliferative activity through dose-dependently inducing cellular apoptosis.

### *2.2.4. In vitro inhibition of the tubulin polymerization*

To obtain an insight into the molecular mechanism of action of these compounds and to investigate whether their antiproliferative activities are related to an interaction with tubulin, the most potent compound **7b** was tested for its *in vitro* ability to inhibit tubulin polymerization using the typical tubulin inhibitor colchicine as the positive control (Wang et al., 2020e). As shown in Fig. 4, after tubulin was incubated with **7b** at various concentrations (3.0, 6.0, 12.5, 25, 50, and 100 μM), the absorbance values decreased compared with the control. Besides, compound **7b** shown a similar inhibitory manner with the positive control colchicine. The results revealed that the effect on the tubulin polymerization positively correlated well with antiproliferative activity, indicating that these 2-phenyl-4,5,6,7-tetrahydro-1*H*-indole derivatives were potent tubulin polymerization inhibitors.

### *2.2.5. Molecular modeling study*

To investigate the possible binding mode of these newly synthesized 2-phenyl-4,5,6,7-tetrahydro-1*H*-indole derivatives with tubulin, molecular docking study of compound **7b** was performed at the colchicine binding site of the tubulin crystal structure (PDB ID: 1SA0) using Autodock vina 1.1.2 (Trott & Olson, 2010). The binding pose of **7b** and tubulin was shown in Fig. 5, and the estimated binding energy was −9.6 kcal·mo $l^{-1}$. As shown in Fig. 5, compound **7b** adopted a "Y-shaped" conformation in the pocket of the tubulin. Compound **7b** located at the hydrophobic pocket, surrounded by the residues A/Ala-180, A/Val-181, B/Leu-248, B/Ala-250, B/Leu-252, B/

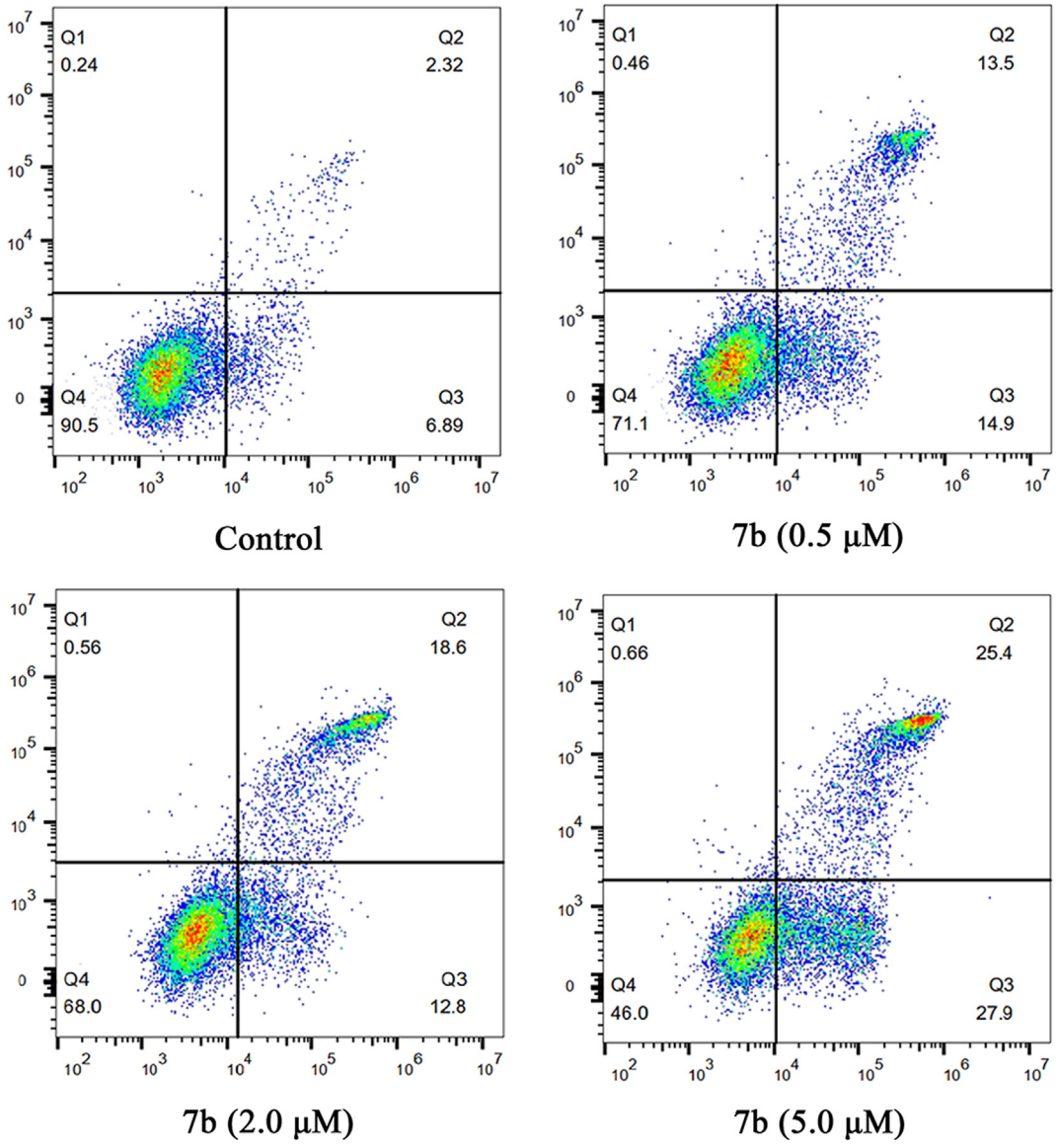


**Fig. 3** Effect of compound **7b** on cell apoptosis in MCF-7 cells. Flow cytometric analysis of apoptotic cells after treatment of MCF-7 cells with **7b** for 24 h. (A) Control; (B) **7b**, 0. 5 μM; (C) **7b**, 2.0 μM; (D) **7b**, 5.0 μM. The diverse cell stages were given as live (Q4), early apoptotic (Q3), late apoptotic (Q2), and necrotic cells (Q1).

Leu-255, B/Ala-316, B/Ala-317, and B/Val-318, forming a strong hydrophobic binding. Detailed analysis showed that the phenyl group of **7b** formed cation-π interactions with the residue Lys-352. It was shown that the residue A/Thr-179 (bond length: 2.2 Å) formed a hydrogen bond with **7b**, which was the main interaction between **7b** and tubulin. All these interactions helped **7b** to anchor in the colchicine binding site of the tubulin.

## 3. Conclusions

In this investigation, we report a novel series of 2-phenyl-4,5,6,7-tetrahydro-1*H*-indole derivatives as potential anti-cancer agents and tubulin polymerization inhibitors. All newly prepared compounds were tested for their antiproliferative activity *in vitro* on the human breast cancer cell line (MCF-7) and human lung adenocarcinoma cell line (A549). The SAR analysis of these compounds revealed that compound **7b** with a 4-methoxyl substituent at the phenylhydrazone moiety exhibited the most potent anticancer activity against MCF-7 and A549 with $IC_{50}$ values of 1.77 ± 0.37 and 3.75 ± 0.11 μM, respectively. Further mechanism studies revealed that **7b** significantly arrested cell cycle at G2/M phase, induced apoptosis with a dose-dependent manner, and inhibited tubulin polymerization. Molecular docking study suggested that **7b** binds well to the colchicine site of tubulin. These preliminary results demonstrate that compound **7b** is a new tubulin

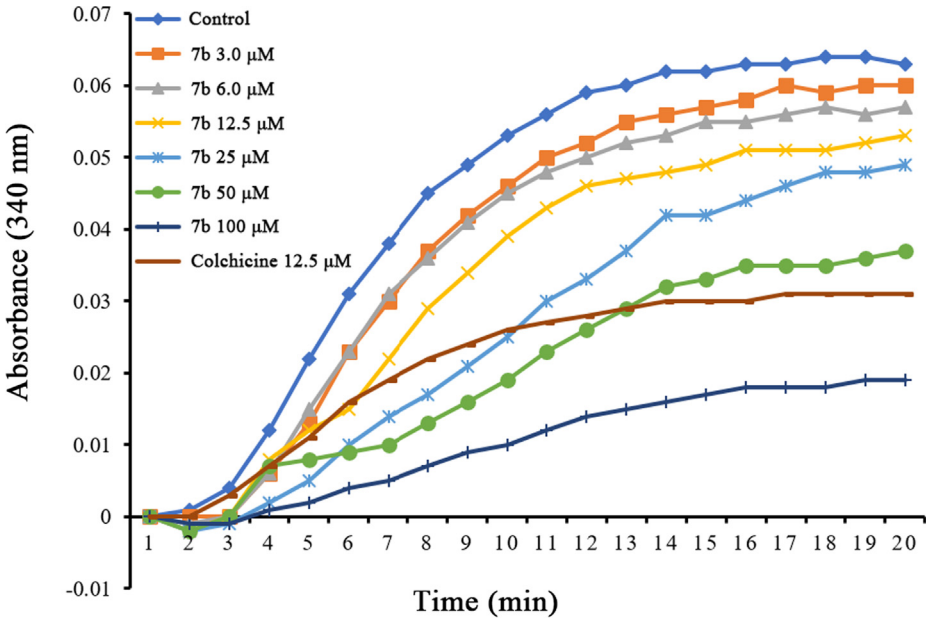


**Fig. 4** Effect of compound **7b** on the *in vitro* tubulin polymerization. Purified tubulin protein and GTP in a reaction buffer incubated at 37 °C in the presence of **7b** (3.0, 6.0, 12.5, 25, 50, and 100 μM), colchicine (12.5 μM) or vehicle (DMSO). Tubulin polymerization reaction was monitored at OD 340 nm every minute at 37 °C over a 20 min period.

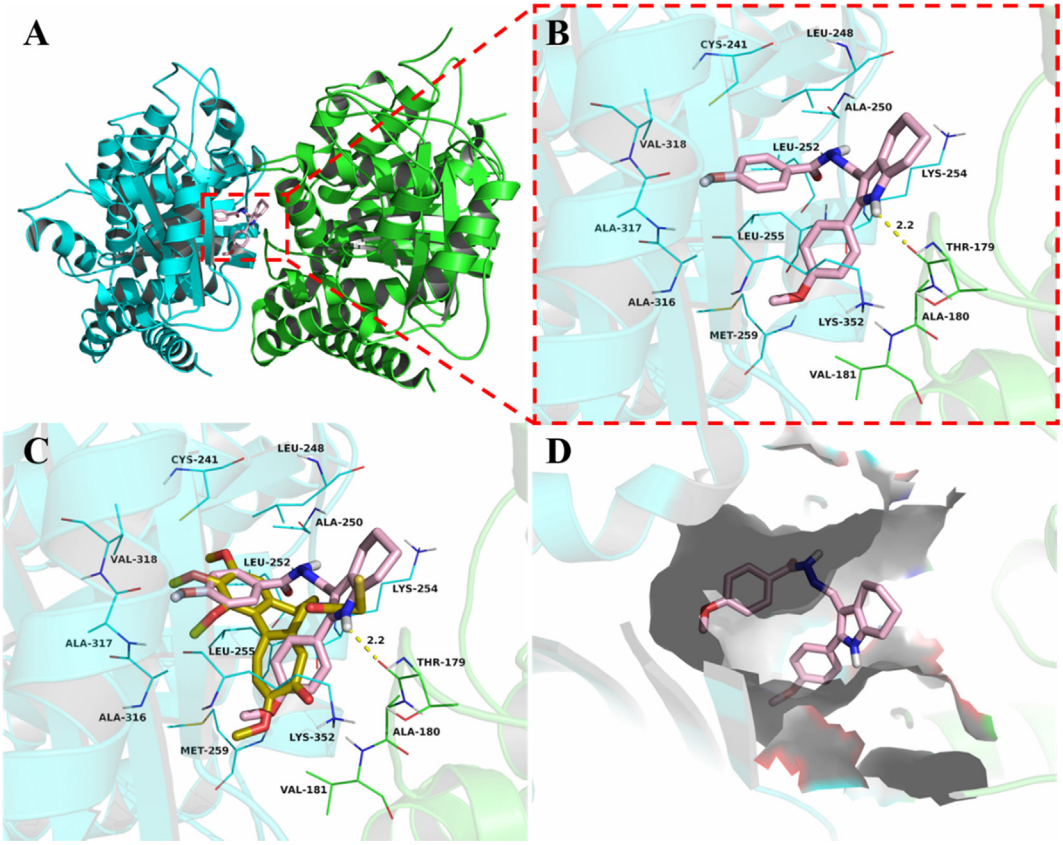


**Fig. 5** Compound **7b** was docked to the colchicine binding site of the tubulin (α: green; β: cyan). (A) The overall structure of tubulin with **7b**. (B) Binding pose of **7b** at colchicine binding site. (C) Superimposed pose of **7b** (pink) and colchicine (yellow-orange) in the binding site. (D) Binding pose of **7b** in the surface of colchicine binding pocket.

polymerization inhibitor and is worthy of further investigation aiming to the development of new potential anticancer agents.

## 4. Experimental section.

### *4.1. Chemistry.*

The starting materials (compound **1**, **2** and **6a-6o**), solvents or reagents were purchased from commercial suppliers. Nuclear magnetic resonance spectra (NMR) were recorded on a JNM spectrometer (400 MHz) with TMS as an external reference and reported in parts per million. High-resolution mass spectra (HRMS) were recorded on Bruker MicroQTOF Ⅱ using ESI method.

#### *4.1.1. 2-(2-(4-Methoxyphenyl)-2-oxoethyl)cyclohexan-1-one (3)*

To a solution of compound **1** (1.0 mmol) in DMF (10 mL) were added and compound **2** (1.0 mmol) and the reacting mixture was stirred at room temperature for 4 h. Then, 100 mL of water was added to the reaction solution and stirred at room temperature for 12 h. The white solid precipitate was collected by filtration and purified by chromatography on silica gel with EtOAc/petroleum ether to give compound **3** as white solid.

#### *4.1.2. 2-(4-Methoxyphenyl)-4,5,6,7-tetrahydro-1H-indole (4)*

A mixture of **3** (1 mmol) and $NH_4Ac$ (5 mmol) in ethanol (10 mL) was stirred at reflux for 1 h. After the completion of the reaction (monitored by TLC), the mixture was poured into water and extracted 3 times for ethyl acetate. The combined organic layers were dried over $Na_2SO_4$ and concentrated under vacuum. The residue was purified by chromatography to give compound **4** as brown solid.

#### *4.1.3. 2-(4-Methoxyphenyl)-4,5,6,7-tetrahydro-1H-indole-3-carbaldehyde (5)*

A mixture of compound **4** (227 mg, 1.0 mmol) and hexamethylenetetramine (281 mg, 2 mmol) in acetic acid (10 mL) was stirred at reflux for 3 h. After the completion of the reaction, the mixture was poured into water (50 mL) and the precipitate was collected by filtration and purified by chromatography to give the key intermediate **5** as yellow solid (88%). $^1$H NMR (DMSO $d_6$, 400 MHz) $\delta$: 1.67–1.74 (m, 4H), 2.50–2.54 (m, 2H), 2.65 (t, 2H, $J$ = 5.6 Hz), 3.80 (s, 3H), 7.03 (d, 2H, $J$ = 8.8 Hz), 7.45 (d, 2H, $J$ = 8.8 Hz), 9.69 (s, 1H), 11.38 (s, 1H).

#### *4.1.4. General procedure for the synthesis of 7*

A mixture of **5** (1.0 mmol) and different benzoyl hydrazines **6** (1.0 mmol) was refluxed in ethanol (10 mL) for 6 h in the presence of one drop of glacial acetic acid. After the completion of the reaction, the solvent was removed under reduced pressure and the residue was purified by silica gel column chromatography (petroleum ether/EtOAc) to give the title compounds **7a-7o**. The spectroscopic and analytical data of these compounds are as follows:

*4.1.4.1. (E)-4-Fluoro-N'-((2-(4-methoxyphenyl)-4,5,6,7-tetrahydro-1H-indol-3-yl)methylene)benzohydrazide (**7a**).* Yellow solid; yield = 72%; $^1$H NMR (DMSO $d_6$, 400 MHz) $\delta$: 1.61–1.77 (m, 4H), 2.49–2.54 (m, 2H), 2.67–2.72 (m, 2H), 3.75 (s, 3H), 6.98 (d, 2H, $J$ = 8.8 Hz), 7.26–7.32 (m, 4H), 7.88–7.91 (m, 2H), 8.40 (s, 1H), 10.89 (s, 1H), 11.24 (s, 1H); $^{13}$C NMR (DMSO $d_6$, 100 MHz) $\delta$: 22.81, 23.21, 23.79, 24.31, 55.75, 113.33, 114.64, 115.65, 115.86, 116.64, 125.37, 128.83, 129.68, 129.77, 130.49, 130.57, 131.09, 133.96, 146.88, 158.92, 161.63; HRMS (ESI) calcd for $[M-H]^-$ $C_{23}H_{21}FN_3O_2^-$: 390.1623 found 390.1653.

*4.1.4.2. (E)-4-methoxy-N'-((2-(4-methoxyphenyl)-4,5,6,7-tetrahydro-1H-indol-3-yl)methylene)benzohydrazide (**7b**).* Brown solid; yield = 84%; $^1$H NMR (DMSO $d_6$, 400 MHz) $\delta$: 1.72–1.75 (m, 4H), 2.56 (t, 2H, $J$ = 6.8 Hz), 2.73 (s, 2H, $J$ = 6.8 Hz), 3.80 (s, 3H), 3.81 (s, 3H), 7.00 (d, 2H, $J$ = 8.4 Hz), 7.02 (d, 2H, $J$ = 8.4 Hz), 7.34 (d, 2H, $J$ = 8.8 Hz), 7.84 (d, 2H, $J$ = 8.4 Hz), 8.44 (s, 1H), 10.88 (s, 1H), 11.14 (s, 1H); $^{13}$C NMR (DMSO $d_6$, 100 MHz) $\delta$: 22.84, 23.25, 23.83, 24.33, 55.76, 55.88, 113.51, 114.04, 114.64, 116.62, 124.80, 125.50, 126.77, 128.74, 129.74, 133.64, 146.21, 158.89, 162.11; HRMS (ESI) calcd for $[M-H]^-$ $C_{24}H_{26}N_3O_3^-$: 404.1980 found 404.1847.

*4.1.4.3. (E)-4-(tert-butyl)-N'-((2-(4-methoxyphenyl)-4,5,6,7-tetrahydro-1H-indol-3-yl)methylene)benzohydrazide (**7c**).* Light yellow solid; yield = 75%; $^1$H NMR (DMSO $d_6$, 400 MHz) $\delta$: 1.26 (s, 9H), 1.69 (s, 4H), 2.51 (s, 2H), 2.69 (s, 2H), 3.75 (s, 3H), 6.97 (d, 2H, $J$ = 8.0 Hz), 7.29 (d, 2H, $J$ = 8.0 Hz), 7.44 (d, 2H, $J$ = 8.0 Hz), 7.74 (d, 2H, $J$ = 8.0 Hz), 8.40 (s, 1H), 10.87 (s, 1H), 11.17 (s, 1H); $^{13}$C NMR (DMSO $d_6$, 100 MHz) $\delta$: 22.83, 23.21, 23.80, 24.32, 31.46, 35.14, 55.72, 113.39, 114.61, 125.39, 125.57, 127.75, 128.77, 129.73, 130.56, 131.87, 133.79, 146.57, 154.47, 158.87, 162.69; HRMS (ESI) calcd for $[M-H]^-$ $C_{27}H_{30}N_3O_2^-$: 428.2344 found 428.2383.

*4.1.4.4. (E)-N'-((2-(4-methoxyphenyl)-4,5,6,7-tetrahydro-1H-indol-3-yl)methylene)benzohydrazide (**7d**).* Yellow solid; yield = 69%; $^1$H NMR (DMSO $d_6$, 400 MHz) $\delta$: 1.70 (s, 4H), 2.52 (s, 2H), 2.70 (s, 2H), 3.75 (s, 3H), 6.98 (d, 2H, $J$ = 8.4 Hz), 7.30 (d, 2H, $J$ = 8.4 Hz), 7.42–7.50 (m, 3H), 7.81–7.83 (m, 2H), 8.41 (s, 1H), 10.88 (s, 1H), 11.24 (s, 1H); $^{13}$C NMR (DMSO $d_6$, 100 MHz) $\delta$: 22.82, 23.22, 23.80, 24.32, 55.74, 113.38, 114.63, 116.65, 125.40, 127.89, 128.81, 129.75, 131.69, 133.88, 134.64, 146.80, 158.90, 162.69; HRMS (ESI) calcd for $[M-H]^-$ $C_{23}H_{22}N_3O_2^-$: 372.1718 found 372.1751.

*4.1.4.5. (E)-4-bromo-N'-((2-(4-methoxyphenyl)-4,5,6,7-tetrahydro-1H-indol-3-yl)methylene)benzohydrazide (**7e**).* Yellow solid; yield = 73%; $^1$H NMR (DMSO $d_6$, 400 MHz) $\delta$: 1.70 (s, 4H), 2.52 (s, 2H), 2.70 (s, 2H), 3.76 (s, 3H), 6.98 (d, 2H, $J$ = 8.8 Hz), 7.31 (d, 2H, $J$ = 8.8 Hz), 7.64 (d, 2H, $J$ = 8.4 Hz), 7.77 (d, 2H, $J$ = 8.4 Hz), 8.41 (s, 1H), 10.82 (s, 1H), 11.23 (s, 1H); $^{13}$C NMR (DMSO $d_6$, 100 MHz) $\delta$: 22.79, 23.20, 23.77, 24.30, 55.75, 113.30, 114.65, 116.64, 125.32, 125.40, 128.86, 129.16, 129.78, 130.03, 130.57, 131.83, 133.68, 134.08, 147.11, 158.94, 161.69; HRMS (ESI) calcd for $[M-H]^-$ $C_{23}H_{21}BrN_3O_2^-$: 450.0823 found 450.0867.

*4.1.4.6. (E)-4-chloro-N'-((2-(4-methoxyphenyl)-4,5,6,7-tetrahydro-1H-indol-3-yl)methylene)benzohydrazide (**7f**).* Light yellow solid; yield = 82%; $^1$H NMR (DMSO $d_6$, 400 MHz) $\delta$: 1.68–1.70 (m, 4H), 2.50–2.51 (m, 2H), 2.65–2.71

(m, 2H), 3.75 (s, 3H), 6.98 (d, 2H, $J$ = 8.8 Hz), 7.29 (d, 2H, $J$ = 8.8 Hz), 7.51 (d, 2H, $J$ = 8.4 Hz), 7.84 (d, 2H, $J$ = 8.4 Hz), 8.40 (s, 1H), 10.91 (s, 1H), 11.30 (s, 1H); $^{13}$C NMR (DMSO $d_6$, 100 MHz) $\delta$: 22.79, 23.20, 23.78, 24.30, 55.75, 113.31, 114.65, 116.65, 125.34, 128.86, 128.90, 129.78, 129.84, 133.33, 134.07, 136.49, 147.10, 158.94, 161.58; HRMS (ESI) calcd for $[M-H]^-$ $C_{23}H_{21}ClN_3O_2^-$: 406.1328 found 406.1367.

*4.1.4.7. (E)-N'-((2-(4-methoxyphenyl)-4,5,6,7-tetrahydro-1H-indol-3-yl)methylene)-4-methylbenzohydrazide (**7g**).* Light yellow solid; yield = 87%; $^1$H NMR (DMSO $d_6$, 400 MHz) $\delta$: 1.68–1.70 (m, 4H), 2.32 (s, 3H), 2.49–2.54 (m, 2H), 2.67–2.72 (m, 2H), 3.75 (s, 3H), 6.98 (d, 2H, $J$ = 8.8 Hz), 7.23 (d, 2H, $J$ = 8.0 Hz), 7.30 (d, 2H, $J$ = 8.8 Hz), 7.72 (d, 2H, $J$ = 8.4 Hz), 8.41 (s, 1H), 10.88 (s, 1H), 11.18 (s, 1H); $^{13}$C NMR (DMSO $d_6$, 100 MHz) $\delta$: 21.51, 22.82, 23.22, 23.80, 24.32, 25.95, 55.74, 113.43, 114.63, 115.02, 116.63, 125.42, 127.90, 128.77, 129.34, 129.74, 131.73, 133.77, 134.31, 141.61, 143.66, 146.52, 158.88, 162.51; HRMS (ESI) calcd for $[M-H]^-$ $C_{24}H_{24}N_3O_2^-$: 386.1874 found 386.1915.

*4.1.4.8. (E)-N'-((2-(4-methoxyphenyl)-4,5,6,7-tetrahydro-1H-indol-3-yl)methylene)-3-methylbenzohydrazide (**7h**).* Light yellow solid; yield = 79%; $^1$H NMR (DMSO $d_6$, 400 MHz) $\delta$: 1.72–1.75 (m, 4H), 2.37 (s, 3H), 2.53–2.58 (m, 2H), 2.71–2.75 (m, 2H), 3.79 (s, 3H), 7.02 (d, 2H, $J$ = 8.8 Hz), 7.34–7.37 (m, 4H), 7.64–7.67 (m, 2H), 8.44 (s, 1H), 10.93 (s, 1H), 11.25 (s, 1H); $^{13}$C NMR (DMSO $d_6$, 100 MHz) $\delta$: 21.49, 22.82, 23.22, 23.80, 24.32, 55.74, 113.40, 114.64, 116.63, 125.09, 125.41, 128.34, 128.72, 128.78, 129.75, 132.27, 133.84, 134.64, 138.08, 146.62, 158.89, 162.77; HRMS (ESI) calcd for $[M-H]^-$ $C_{24}H_{24}N_3O_2^-$: 386.1874 found 386.1919.

*4.1.4.9. (E)-3-chloro-N'-((2-(4-methoxyphenyl)-4,5,6,7-tetrahydro-1H-indol-3-yl)methylene)benzohydrazide (**7i**).* Yellow solid; yield = 82%; $^1$H NMR (DMSO $d_6$, 400 MHz) $\delta$: 1.72–1.75 (m, 4H), 2.54–2.58 (m, 2H), 2.71–2.76 (m, 2H), 3.80 (s, 3H), 7.03 (d, 2H, $J$ = 8.8 Hz), 7.34 (d, 2H, $J$ = 8.8 Hz), 7.53 (t, 1H, $J$ = 8.0 Hz), 7.61–7.63 (m, 1H), 7.82 (d, 1H, $J$ = 8.0 Hz), 7.91 (s, 1H), 8.44 (s, 1H), 10.97 (s, 1H), 11.37 (s, 1H); $^{13}$C NMR (DMSO $d_6$, 100 MHz) $\delta$: 22.80, 23.20, 23.78, 24.30, 55.76, 113.27, 114.66, 116.66, 125.32, 126.76, 127.56, 128.87, 129.80, 130.87, 131.54, 133.64, 134.16, 136.63, 147.24, 158.96, 161.16; HRMS (ESI) calcd for $[M-H]^-$ $C_{23}H_{21}ClN_3O_2^-$: 406.1328 found 406.1376.

*4.1.4.10. (E)-N'-((2-(4-methoxyphenyl)-4,5,6,7-tetrahydro-1H-indol-3-yl)methylene)-3-nitrobenzohydrazide (**7j**).* Orange solid; yield = 76%; $^1$H NMR (DMSO $d_6$, 400 MHz) $\delta$: 1.74 (s, 4H), 2.56 (s, 2H), 2.75 (s, 2H), 3.80 (s, 3H), 7.04 (d, 2H, $J$ = 8.8 Hz), 7.35 (d, 2H, $J$ = 8.8 Hz), 7.80 (t, 1H, $J$ = 8.0 Hz), 8.31 (d, 1H, $J$ = 8.0 Hz), 8.39 (d, 1H, $J$ = 8.0 Hz), 8.47 (s, 1H), 8.70 (s, 1H), 11.00 (s, 1H), 11.60 (s, 1H); $^{13}$C NMR (DMSO $d_6$, 100 MHz) $\delta$: 22.80, 23.19, 23.77, 24.30, 55.77, 113.23, 114.69, 116.68, 122.55, 125.28, 126.35, 128.93, 129.72, 129.86, 130.65, 134.56, 136.04, 147.67, 148.24, 159.02, 160.44; HRMS (ESI) calcd for $[M-H]^-$ $C_{23}H_{21}N_4O_4^-$: 417.1568 found 417.1611.

*4.1.4.11. (E)-3,4,5-trimethoxy-N'-((2-(4-methoxyphenyl)-4,5,6,7-tetrahydro-1H-indol-3-yl)methylene)benzohydrazide (**7k**).* Brown solid; yield = 78%; $^1$H NMR (DMSO $d_6$, 400 MHz) $\delta$: 1.72–1.75 (m, 4H), 2.56 (s, 2H), 2.73 (s, 2H), 3.70 (s, 3H), 3.79 (s, 3H), 3.83 (s, 6H), 7.02 (d, 2H, $J$ = 8.8 Hz), 7.17 (s, 2H), 7.34 (d, 2H, $J$ = 8.8 Hz), 8.42 (s, 1H), 10.95 (s, 1H), 11.17 (s, 1H); $^{13}$C NMR (DMSO $d_6$, 100 MHz) $\delta$: 22.81, 23.21, 23.81, 24.30, 55.76, 56.58, 60.63, 105.46, 113.39, 114.69, 116.65, 125.40, 128.81, 129.82, 133.90, 140.44, 146.83, 153.10, 158.96, 162.27; HRMS (ESI) calcd for $[M-H]^-$ $C_{26}H_{28}N_3O_5^-$: 462.2034 found 462.2075.

*4.1.4.12. (E)-2-amino-N'-((2-(4-methoxyphenyl)-4,5,6,7-tetrahydro-1H-indol-3-yl)methylene)benzohydrazide (**7l**).* Yellow solid; yield = 81%; $^1$H NMR (DMSO $d_6$, 400 MHz) $\delta$: 1.69 (s, 4H), 2.51 (s, 2H), 2.69 (s, 2H), 3.75 (s, 3H), 6.28 (s, 2H), 6.47 (t, 1H, $J$ = 8.0 Hz), 6.65 (d, 1H, $J$ = 8.0 Hz), 6.97 (d, 2H, $J$ = 8.8 Hz), 7.10 (t, 1H, $J$ = 8.0 Hz), 7.29 (d, 2H, $J$ = 8.8 Hz), 7.43 (d, 1H, $J$ = 8.0 Hz), 8.37 (s, 1H), 10.36 (s, 1H), 11.04 (s, 1H); $^{13}$C NMR (DMSO $d_6$, 150 MHz) $\delta$: 22.78, 23.18, 23.76, 24.30, 55.68, 113.46, 114.55, 114.94, 116.53, 116.62, 125.47, 128.51, 128.65, 129.63, 131.49, 132.10, 132.51, 133.49, 145.91, 150.20, 158.77; HRMS (ESI) calcd for $[M-H]^-$ $C_{23}H_{23}N_4O_2^-$: 387.1826 found 387.1887.

*4.1.4.13. (E)-4-amino-N'-((2-(4-methoxyphenyl)-4,5,6,7-tetrahydro-1H-indol-3-yl)methylene)benzohydrazide (**7m**).* Yellow solid; yield = 74%; $^1$H NMR (DMSO $d_6$, 400 MHz) $\delta$: 1.67–1.70 (m, 4H), 2.51 (s, 2H), 2.67 (s, 2H), 3.75 (s, 3H), 5.64 (s, 2H), 6.49 (d, 2H, $J$ = 8.4 Hz), 6.97 (d, 2H, $J$ = 8.4 Hz), 7.29 (d, 2H, $J$ = 8.4 Hz), 7.55 (d, 2H, $J$ = 8.4 Hz), 8.37 (s, 1H), 10.83 (s, 1H), 10.86 (s, 1H); $^{13}$C NMR (DMSO $d_6$, 100 MHz) $\delta$: 22.83, 23.23, 23.83, 24.31, 55.72, 113.08, 114.60, 116.56, 120.87, 125.54, 128.66, 129.46, 129.65, 133.24, 145.22, 152.25, 158.77, 162.73; HRMS (ESI) calcd for $[M-H]^-$ $C_{23}H_{23}N_4O_2^-$: 387.1826 found 387.1879.

*4.1.4.14. (E)-4-hydroxy-N'-((2-(4-methoxyphenyl)-4,5,6,7-tetrahydro-1H-indol-3-yl)methylene)benzohydrazide (**7n**).* Brown solid; yield = 80%; $^1$H NMR (DMSO $d_6$, 400 MHz) $\delta$: 1.68 (s, 4H), 2.51 (s, 2H), 2.68 (s, 2H), 3.75 (s, 3H), 6.76 (d, 2H, $J$ = 8.0 Hz), 6.97 (d, 2H, $J$ = 8.0 Hz), 7.29 (d, 2H, $J$ = 8.0 Hz), 7.69 (d, 2H, $J$ = 8.0 Hz), 8.38 (s, 1H), 9.98 (s, 1H), 10.86 (s, 1H), 11.04 (s, 1H); $^{13}$C NMR (DMSO $d_6$, 100 MHz) $\delta$: 22.84, 23.24, 23.83, 24.33, 55.74, 113.53, 114.61, 115.33, 116.59, 125.18, 125.51, 128.70, 129.70, 129.82, 133.50, 145.91, 158.84, 160.65, 162.34; HRMS (ESI) calcd for $[M-H]^-$ $C_{23}H_{22}N_3O_3^-$: 388.1667 found 388.1702.

*4.1.4.15. (E)-3-bromo-N'-((2-(4-methoxyphenyl)-4,5,6,7-tetrahydro-1H-indol-3-yl)methylene)benzohydrazide (**7o**).* Yellow solid; yield = 83%; $^1$H NMR (DMSO $d_6$, 400 MHz) $\delta$: 1.65–1.65 (m, 4H), 2.50 (s, 2H), 2.68 (s, 2H), 3.74 (s, 3H), 6.97 (d, 2H, $J$ = 8.8 Hz), 7.29 (d, 2H, $J$ = 8.8 Hz), 7.41 (t, 1H, $J$ = 8.0 Hz), 7.68–7.71 (m, 1H), 7.80 (d, 1H, $J$ = 8.0 Hz), 7.98–7.98 (m, 1H), 8.38 (s, 1H), 10.90 (s, 1H), 11.32 (s, 1H); $^{13}$C NMR (DMSO $d_6$, 100 MHz) $\delta$: 22.78, 23.18, 23.77, 24.28, 55.75, 113.25, 114.67, 116.67, 122.14, 125.28, 127.13, 128.90, 129.79, 130.38, 131.15, 134.20, 134.46, 136.77, 147.31, 158.96, 161.15; HRMS (ESI) calcd for $[M-H]^-$ $C_{23}H_{21}BrN_3O_2^-$: 450.0823 found 450.0877.

### *4.2. Cell proliferation and cytotoxicity assays*

Cell proliferation and cytotoxicity of these newly synthesized compounds were evaluated following our previous reports

using CCK-8 assay (Wang et al., 2021). Briefly, cells (MCF-7, A549 and LO2) were seeded in 96-well plates at $1 \times 10^4$ cells/well and cultured in RPMI-1640 with 10% fetal bovine serum for 24 h. Then, the cells were treated with different concentrations (0.3125, 0.625, 1.25, 2.5, 5.0, 10 and 20 μM) of tested compounds or standard drugs for 48 h. After incubation, cell viability was determined by the CCK-8 method after incubation. The cell proliferation and cytotoxicity were expressed as the $IC_{50}$ values.

### 4.3. Cell cycle assay

Human breast cancer cells (MCF-7) were treated with DMSO or different concentrations of compound **7b** (0.625, 1.25 and 2.5 μM) for 24 h. After incubation, the cells were collected, washed with PBS, and fixed by ice-cold ethanol (75%) at 4 °C overnight. Subsequently, cells were then washed, treated using RNase (50 μg/mL) for 30 min at 37 °C, and stained with propidium iodide. The DNA content of the cells was analyzed using a flow cytometry.

### 4.4. Cell apoptosis assay

After treatment with different concentrations of **7b** (0.5, 2.0 and 5.0 μM) and vehicle for 24 h, MCF-7 cells were harvested and incubated with 5 μL Annexin-V/FITC in binding buffer (containing 140 mM NaCl, 10 mM HEPES, 2.5 mM $CaCl_2$, pH 7.4) and 10 μL PI staining solution at room temperature for 15 min. Thereafter, the stained cells were analyzed by flow cytometry.

### 4.5. Tubulin polymerization assay

Tubulin protein was purified from pig brain, and experimental details for tubulin polymerization assay were reported in our previous work (Wang et al., 2018b). The purified tubulin protein was incubated with different concentrations of 7b, colchicine) or DMSO in PEM buffer (100 mM PIPES, 1 mM MgCl2, and 1 mM EGTA) containing 1 mM GTP and 5 % glycerol. The absorbance value at 340 nm was monitored by a SPECTRA MAX 190 (Molecular Device) spectrophotometer. The plateau absorbance values were used for calculations.

### 4.6. Molecular modeling study

According to our previous work, molecular modeling study was performed by Autodock vina 1.1.2. The x-ray crystal structure of tubulin (PDB ID: 1SA0) was downloaded from the Protein Data Bank (PDB). In brief, the search grid of the tubulin was identified as center_x: 118.921, center_y: 89.718, and center_z: 5.932 with dimensions size_x: 15, size_y: 15, and size_z: 15. The value of exhaustiveness was set to 20. The top-score docking poses were selected and visually analyzed using PyMoL 1.7.6 software (www.pymol.org).

### 4.7. Statistical analysis

All experiments were carried out at least in three independent trials. The experimental data were expressed as the mean ± standard deviation.

## Acknowledgements

This work was supported by One Thousand Talents Program of Guizhou Province (the fifth group, [2019]4), Academic New Seedling Project of Guizhou Medical University (19NSP030).

## Appendix A. Supplementary material

Supplementary data to this article can be found online at https://doi.org/10.1016/j.arabjc.2021.103504.

## References

Ahmad, S., Alam, O., Naim, M.J., Shaquiquzzaman, M., Alam, M. M., Iqbal, M., 2018. Pyrrole: An insight into recent pharmacological advances with structure activity relationship. Eur. J. Med. Chem. 157, 527–561. https://doi.org/10.1016/j.ejmech.2018.08.002.

Amos, L.A., 2004. Microtubule structure and its stabilisation. Organic Biomol. Chem. 2 (15), 2153–2160. https://doi.org/10.1039/b403634d.

Andreev, I.A., Manvar, D., Barreca, M.L., Belov, D.S., Basu, A., Sweeney, N.L., Ratmanova, N.K., Lukyanenko, E.R., Manfroni, G., Cecchetti, V., Frick, D.N., Altieri, A., Kaushik-Basu, N., Kurkin, A.V., 2015. Discovery of the 2-phenyl-4,5,6,7-Tetrahydro-1H-indole as a novel anti-hepatitis C virus targeting scaffold. Eur. J. Med. Chem. 96, 250–258. https://doi.org/10.1016/j.ejmech.2015.04.022.

Downing, K.H., Nogales, E., 1998a. Tubulin and microtubule structure. Curr. Opin. Cell Biol. 10 (1), 16–22. https://doi.org/10.1016/s0955-0674(98)80082-3.

Downing, K.H., Nogales, E., 1998b. Tubulin structure: insights into microtubule properties and functions. Curr. Opin. Struct. Biol. 8 (6), 785–791. https://doi.org/10.1016/s0959-440x(98)80099-7.

Dumontet, C., Jordan, M.A., 2010. Microtubule-binding agents: a dynamic field of cancer therapeutics. Nat. Rev. Drug Discovery 9 (10), 790–803. https://doi.org/10.1038/nrd3253.

Fatahala, S.S., Shalaby, E.A., Kassab, S.E., Mohamed, M.S., 2015. A Promising Anti-Cancer and Anti-Oxidant Agents Based on the Pyrrole and Fused Pyrrole: Synthesis, Docking Studies and Biological Evaluation. Anti-Cancer Agents Med. Chem. 15 (4), 517–526. https://doi.org/10.2174/1871520615666150105113946.

Gulcin, I., Trofimov, B., Kaya, R., Taslimi, P., Sobenina, L., Schmidt, E., Petrova, O., Malysheva, S., Gusarova, N., Farzaliyev, V., Sujayev, A., Alwasel, S., Supuran, C.T., 2020. Synthesis of nitrogen, phosphorus, selenium and sulfur-containing heterocyclic compounds - Determination of their carbonic anhydrase, acetylcholinesterase, butyrylcholinesterase and alpha-glycosidase inhibition properties. Bioorg. Chem. 103. https://doi.org/10.1016/j.bioorg.2020.104171.

Honore, S., Pasquier, E., Braguer, D., 2005. Understanding microtubule dynamics for improved cancer therapy. Cell. Mol. Life Sci. 62 (24), 3039–3056. https://doi.org/10.1007/s00018-005-5330-x.

Jordan, M.A., Wendell, K., Gardiner, S., Derry, W.B., Copp, H., Wilson, L., 1996. Mitotic block induced in HeLa cells by low concentrations of paclitaxel (taxol) results in abnormal mitotic exit and apoptotic cell death. Cancer Res. 56 (4), 816–825.

Jordan, M.A., Wilson, L., 2004. Microtubules as a target for anticancer drugs. Nat. Rev. Cancer 4 (4), 253–265. https://doi.org/10.1038/nrc1317.

Li, L., Jiang, S.B., Li, X.X., Liu, Y., Su, J., Chen, J.J., 2018. Recent advances in trimethoxyphenyl (TMP) based tubulin inhibitors targeting the colchicine binding site. Eur. J. Med. Chem. 151, 482–494. https://doi.org/10.1016/j.ejmech.2018.04.011.

Li, W., Sun, H., Xu, S., Zhu, Z., Xu, J., 2017. Tubulin inhibitors targeting the colchicine binding site: A perspective of privileged

structures. Future Med. Chem. 9 (15), 1765–1794. https://doi.org/10.4155/fmc-2017-0100.

Mustafa, M., Anwar, S., Elgamal, F., Ahmed, E. R., & Aly, O. M. (2019). Potent combretastatin A-4 analogs containing 1,2,4-triazole: Synthesis, antiproliferative, anti-tubulin activity, and docking study. *European Journal of Medicinal Chemistry, 183*, 111697. https://doi.org/ 10.1016/j.ejmech.2019.111697.

Naik, M., Ghorpade, S., Jena, L.K., Gorai, G., Narayan, A., Guptha, S., Sharma, S., Dinesh, N., Kaur, P., Nandishaiah, R., Bhat, J., Balakrishnan, G., Humnabadkar, V., Ramachandran, V., Naviri, L.K., Khadtare, P., Panda, M., Iyer, P.S., Chatterji, M., 2014. 2-Phenylindole and Arylsulphonamide: Novel Scaffolds Bactericidal against Mycobacterium tuberculosis. ACS Med. Chem. Lett. 5 (9), 1005–1009. https://doi.org/10.1021/ml5001933.

Patil, R., Patil, S.A., Beaman, K.D., Patil, S.A., 2016. Indole molecules as inhibitors of tubulin polymerization: potential new anticancer agents, an update (2013–2015). Future Med. Chem. 8 (11), 1291–1316. https://doi.org/10.4155/fmc-2016-0047.

Sang, Y.-L., Zhang, W.-M., Lv, P.-C., Zhu, H.-L., 2017. Indole-based, antiproliferative agents targeting tublin polymerizaton. Curr. Top. Med. Chem. 17 (2), 120–137. https://doi.org/10.2174/1568026616666160530154812.

Singh, N., Singh, S., Kohli, S., Singh, A., Asiki, H., Rathee, G., Chandra, R., Anderson, E.A., 2021. Recent progress in the total synthesis of pyrrole-containing natural products (2011–2020). Org. Chem. Front. https://doi.org/10.1039/d0qo01574a.

Singh, T.P., Singh, O.M., 2018. Recent Progress in Biological Activities of Indole and Indole Alkaloids. Mini-Reviews in Medicinal Chemistry 18 (1), 9–25. https://doi.org/10.2174/1389557517666170807123201.

Sravanthi, T.V., Manju, S.L., 2016. Indoles - A promising scaffold for drug development. Eur. J. Pharm. Sci. 91, 1–10. https://doi.org/10.1016/j.ejps.2016.05.025.

Stanton, R.A., Gernert, K.M., Nettles, J.H., Aneja, R., 2011. Drugs That Target Dynamic Microtubules: A New Molecular Perspective. Med. Res. Rev. 31 (3), 443–481. https://doi.org/10.1002/med.20242.

Sun, L., Tran, N., Liang, C.X., Hubbard, S., Tang, F., Lipson, K., Schreck, R., Zhou, Y., McMahon, G., Tang, C., 2000. Identification of substituted 3- (4,5,6,7-tetrahydro-1H-indol-2-yl)methylene - 1,3-dihydroindol-2-ones as growth factor receptor inhibitors for VEGF-R2 (Flk-1/KDR), FGF-R1, and PDGF-R beta tyrosine kinases. J. Med. Chem. 43 (14), 2655–2663. https://doi.org/10.1021/jm9906116.

Sunil, D., Kamath, P.R., 2016. Indole based tubulin polymerization inhibitors: An update on recent developments. Mini-Reviews in Medicinal Chemistry 16 (18), 1470–1499. https://doi.org/10.2174/1389557516666160505115324.

Trott, O., Olson, A.J., 2010. Software news and update AutoDock Vina: Improving the speed and accuracy of docking with a new scoring function, efficient optimization, and multithreading. J. Comput. Chem. 31 (2), 455–461. https://doi.org/10.1002/jcc.21334.

Vojacek, S., Schulig, L., Wossner, N., Geist, N., Langel, W., Jung, M., Schade, D., Link, A., 2019. Tetrahydroindoles as Multipurpose Screening Compounds and Novel Sirtuin Inhibitors. ChemMedChem 14 (8), 853–864. https://doi.org/10.1002/cmdc.201900054.

Wan, Y.C., Li, Y.H., Yan, C.X., Yan, M., Tang, Z.L., 2019. Indole: A privileged scaffold for the design of anti-cancer agents. Eur. J. Med. Chem. 183. https://doi.org/10.1016/j.ejmech.2019.111691.

Wang, G., Fan, M., Liu, W., He, M., Li, Y., Peng, Z., 2021. Synthesis, biological evaluation and molecular docking investigation of new sulphonamide derivatives bearing naphthalene moiety as potent tubulin polymerisation inhibitors. J. Enzyme Inhib. Med. Chem. 36 (1), 1402–1410. https://doi.org/10.1080/14756366.2021.1943378.

Wang, G., Li, C., He, L., Lei, K., Wang, F., Pu, Y., Yang, Z., Cao, D., Ma, L., Chen, J., Sang, Y., Liang, X., Xiang, M., Peng, A., Wei, Y., Chen, L., 2014. Design, synthesis and biological evaluation of a series of pyrano chalcone derivatives containing indole moiety as novel anti-tubulin agents. Bioorg. Med. Chem. 22 (7), 2060–2079. https://doi.org/10.1016/j.bmc.2014.02.028.

Wang, G., Liu, W., Gong, Z., Huang, Y., Li, Y., Peng, Z., 2020a. Design, synthesis, biological evaluation and molecular docking studies of new chalcone derivatives containing diaryl ether moiety as potential anticancer agents and tubulin polymerization inhibitors. Bioorg. Chem. 95,. https://doi.org/10.1016/j.bioorg.2019.103565 103565.

Wang, G., Liu, W., Gong, Z., Huang, Y., Li, Y., Peng, Z., 2020b. Synthesis, biological evaluation, and molecular modelling of new naphthalene-chalcone derivatives as potential anticancer agents on MCF-7 breast cancer cells by targeting tubulin colchicine binding site. J. Enzyme Inhib. Med. Chem. 35 (1), 139–144. https://doi.org/10.1080/14756366.2019.1690479.

Wang, G., Liu, W., Huang, Y., Li, Y., Peng, Z., 2020c. Design, synthesis and biological evaluation of isoxazole-naphthalene derivatives as anti-tubulin agents. Arabian J. Chem. 13 (6), 5765–5775. https://doi.org/10.1016/j.arabjc.2020.04.014.

Wang, G., Liu, W., Peng, Z., Huang, Y., Gong, Z., Li, Y., 2020d. Design, synthesis, molecular modeling, and biological evaluation of pyrazole-naphthalene derivatives as potential anticancer agents on MCF-7 breast cancer cells by inhibiting tubulin polymerization. Bioorg. Chem. 103,. https://doi.org/10.1016/j.bioorg.2020.104141 104141.

Wang, G., Liu, W., Tang, J., Ma, X., Gong, Z., Huang, Y., Li, Y., Peng, Z., 2020e. Design, synthesis, and anticancer evaluation of benzophenone derivatives bearing naphthalene moiety as novel tubulin polymerization inhibitors. Bioorg. Chem. 104,. https://doi.org/10.1016/j.bioorg.2020.104265 104265.

Wang, G., Peng, Z., Zhang, J., Qiu, J., Xie, Z., Gong, Z., 2018a. Synthesis, biological evaluation and molecular docking studies of aminochalcone derivatives as potential anticancer agents by targeting tubulin colchicine binding site. Bioorg. Chem. 78, 332–340. https://doi.org/10.1016/j.bioorg.2018.03.028.

Wang, G., Qiu, J., Xiao, X., Cao, A., Zhou, F., 2018b. Synthesis, biological evaluation and molecular docking studies of a new series of chalcones containing naphthalene moiety as anticancer agents. Bioorg. Chem. 76, 249–257. https://doi.org/10.1016/j.bioorg.2017.11.017.

Xia, L.Y., Zhang, Y.L., Yang, R., Wang, Z.C., Lu, Y.D., Wang, B.Z., Zhu, H.L., 2020. Tubulin Inhibitors Binding to Colchicine-Site: A Review from 2015 to 2019. Curr. Med. Chem. 27 (40), 6787–6814. https://doi.org/10.2174/0929867326666191003154051.